5. Nitrous Oxide and Halocarbon Division

T.M. THOMPSON (EDITOR), J.W. ELKINS, J.H. BUTLER, S.A. MONTZKA, R.C. MYERS, T.J. BARING, S.O. CUMMINGS, G.S. DUTTON, J.M. GILLIGAN, A.H. HAYDEN, J.M. LOBERT, T.H. SWANSON, D.F. HURST, AND C.M. VOLK

5.1. CONTINUING PROGRAMS

5.1.1. FLASK SAMPLES

Air samples were collected in pairs and analyzed as in the past with one change. In mid-June, flasks started being humidified by filling them with air flowing through a bubbler prior to their being returned to the field sites. This conditioning step is an attempt to passivate the flask walls and minimize surface chemistry for compounds like carbon tetrachloride (CCl_4). Filling instructions were revised and, therefore, flasks are purged 50% longer. The efficacy of these changes is currently being assessed.

Other minor program changes also instituted in June included: (1) using flow meters with the larger flasks during filling so that flushing rates are equal, (2) conducting field site pump performance tests periodically, and (3) checking flask pressures after filling and before analysis on each instrument. More 0.85 and 2.5 L flasks were added; therefore, instruments such as the gas chromatograph-mass spectrometer (GC-MS) were guaranteed sufficient air for analyses.

A maintenance trip was made to Alert, Northwest Territories, Canada, in May to install an air sampling inlet system [*Montzka et al.*, 1992]. The air inlets are at 10 m and 5 m on the north tower. Flasks are currently filled only from the highest inlet. SPO is the other field site where flasks are filled through this type of inlet system.

A year of analyzing the flask air samples on the original electron capture-gas chromatograph (EC-GC) and the Autoflask system is complete. The Autoflask system is patterned after the Radiatively Important Trace Species (RITS) GC in situ system [*Montzka et al.*, 1992]. This comparison showed some weaknesses in the Autoflask flask inlet plumbing and system control software. Necessary changes were made, and an additional period of overlapping analyses will be done before the old GC is retired from service.

Chlorofluorocarbon (CFC) -11 and -12 concentration growth rates continue to decrease as their expected usage diminished [*Elkins et al.*, 1993]. In 1993 the CFC-11 growth rate was about 1 ppt yr^{-1} with CFC-12 being 10 ppt yr^{-1} (Figure 5.1).

The growth rate of nitrous oxide (N_2O) has decreased since 1991 from about 1 ppb yr^{-1} to 0.5 ppb yr^{-1}. The yearly global means of measurements from flasks collected at seven sites show that mixing ratios of N_2O appear to have leveled off in 1993 (Figure 5.2). The cause of this decrease in the growth rate is unknown and may be the result of many mitigating factors. Worldwide use of fertilizer has decreased by over 10% which will lessen its source of N_2O. Since the eruption of Mt. Pinatubo in June 1991, northern hemispheric temperatures have decreased by 0.5°C; this could reduce the N_2O amount produced by bacteria that are strongly influenced by temperature change. Since the summer of 1990 through the end of 1993, the SOI was consistently negative. A large negative anomaly (<-1) indicates a warming event in the tropical ocean that usually means less equatorial upwelling and less flux of deep water N_2O into the atmosphere. Two such events were recorded in the summer of 1991 and summer of 1992 through the spring of 1993.

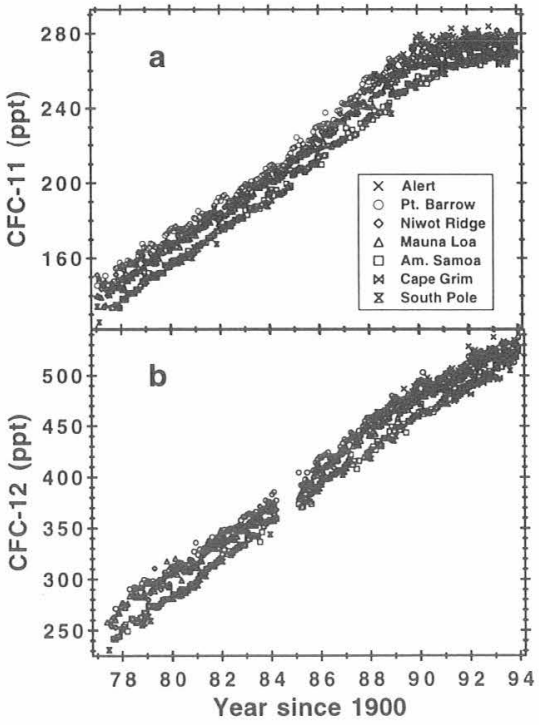

Fig. 5.1. Monthly means of atmospheric mixing ratios measured from flasks collected at the seven NOAH flask network sites for (*a*) CFC-11 and (*b*) CFC-12. Values are reported as dry mole fractions [*Elkins et al.*, 1993] in parts-per-trillion (ppt). A color figure is available from the authors.

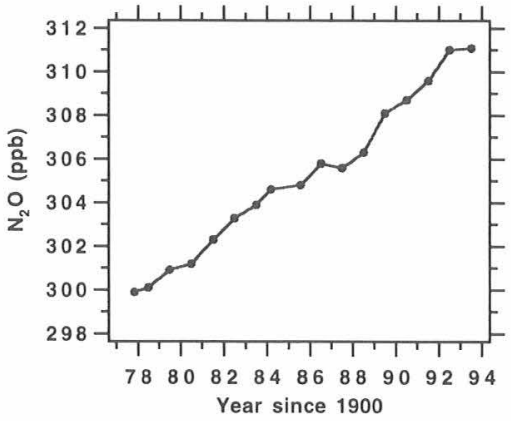

Fig. 5.2. Yearly global means of atmospheric N_2O mixing ratios collected at the seven NOAH flask network sites. Values are reported as dry mole fractions in parts-per-billion (ppb).

5.1.2. RITS Continuous Gas Chromatograph Systems

During scheduled maintenance trips to the field sites, calibration tank regulator heaters and automatic shut-off solenoid valves were installed. The regulator heaters operate at 60°C and reduce contamination buildup. The solenoid valves are in-line between the two calibration tank regulators and the stream select valve. If a power outage occurs, the solenoid valves close preventing the possible loss of valuable calibration gases.

Electron capture detectors (ECDs) at BRW, NWR, and SMO had to be replaced during 1993. In all cases the channel that measures CFC-11, CFC-113, CH_3CCl_3, and CCl_4 was the one that had baseline frequency gradually increase from a nominal 100 Hz to well over 1000 Hz. The method of cleaning a detector by flowing H_2 through it at normal operating temperature for 24 hours or more did not improve the background frequency.

Calibration cylinder gases at the field sites typically last about 1.5 years. The ratios of the chromatogram areas for all components in the two calibration tanks are monitored for possible drift. When a calibration cylinder's pressure falls below 1.3 MPa it is replaced. The new tank components' mixing ratios were determined with a precision better than 0.5%. For a chemical like N_2O, whose growth rate in the atmosphere is small being similar to the calibration precision, step jumps can occur in the data when calibration gases are changed. A technique to counteract this problem and also attempt to detect drift in the working standards was instituted in 1993. Two well-calibrated gas standards (round robins), one at ambient and the other at ~10% below ambient mixing ratios, were taken to the field sites over a period of a month and analyzed in place of outside air for 2 days. This intercalibration documented working standard mixing ratios over a span of a few weeks at all of the sites except SPO. GC linearity and precision were also determined. By continuing this procedure quarterly, problems associated with standards' drift and instrument vagaries should be minimized. Some adjustments in the data base will probably be required as this method becomes routine and attempts are made to back correct the data based on better defined instrument calibration curves.

Monthly mean data for CFC-11 are pictured in Figure 5.3. The marked decrease in growth rate is obvious and comparable to that determined from the longer flask record. Likewise, CFC-12 data are shown in Figure 5.4 and correlate well with the flask mixing ratios. The data for N_2O (Figure 5.5) were adjusted because of the round robin intercalibrations. These data are preliminary and may require further adjustment as the

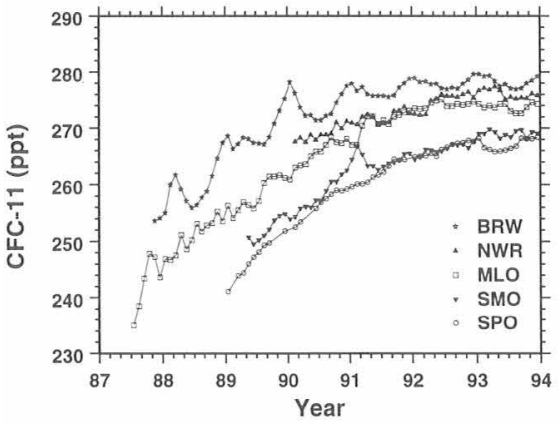

Fig. 5.3. Monthly average CFC-11 mixing ratios in ppt from the in situ GCs.

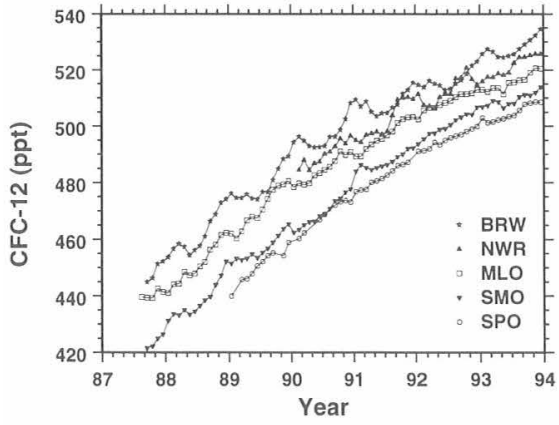

Fig. 5.4. Monthly average CFC-12 mixing ratios in ppt from the in situ GCs.

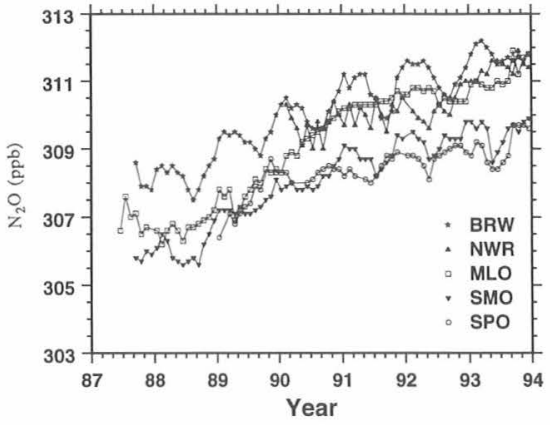

Fig. 5.5. Monthly average N_2O mixing ratios in ppb from the in situ GCs. New calibration and water vapor corrections were applied.

intercalibrations continue. NWR data were corrected for the period when the Nafion drier was not installed. This removed or reduced the annual cycle seen in previously published results.

5.1.3. Low Electron Attachment Potential Species (LEAPS)

Measurements of halons H-1301 and H-1211, CFC-113, CH_3Br, and CH_3Cl continued with the new LEAPS GC system throughout 1993. Except for H-1301, these compounds were also measured by GC-MS throughout the year. Halon data from the EC-GC installed in April 1992 are extremely precise (within 0.01-0.03 ppt on average), although the response for H-1211 is still non-linear on the new system. By mid-1992, the data suggested a substantial slowdown in the growth of the two halons in the atmosphere [*Butler et al.*, 1992]. However, the recent values, which are more frequent and more precise and that extend the data set from 5 to 7 years, indicate that the slowdown may not be as substantial as previously reported. During 1993, atmospheric H-1211 increased at 0.1-0.2 ppt yr^{-1} (3-7% yr^{-1}), and H-1301 increased at about 0.2 ppt yr^{-1} (10% yr^{-1}). At the end of 1993, the latitudinally weighted, mean mole fractions of H-1301 and H-1211 are 2.1 and 3.1 ppt, representing 25-35% of organic bromine in the remote atmosphere (Figure 5.6).

Because of a numerical error in the calculation routines, previously reported values for H-1211 should be adjusted upward by 15%. Reanalyses of cylinder SRL-K-009288, an Aculife-treated steel cylinder that has served as the principal secondary standard for all reported halon values, have agreed within ±0.2 ppt for each of the halons over 3-5 years. Earlier calibrations, however, were not as precise as those done since early 1992, therefore it is difficult at this time to determine

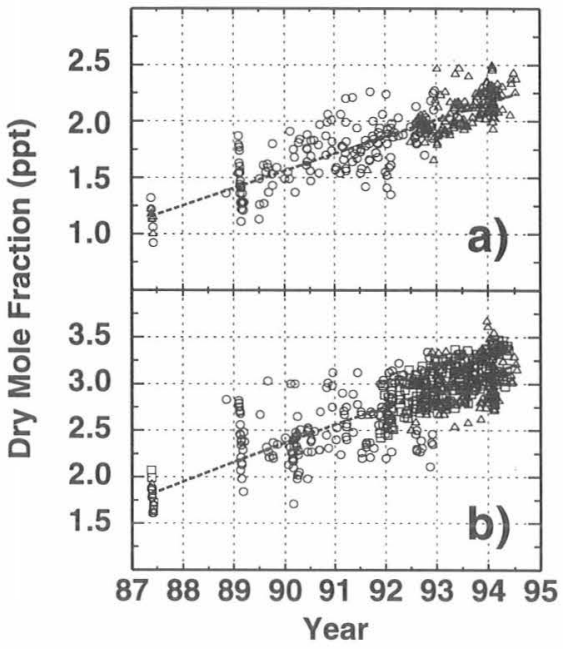

Fig. 5.6. Composite plots of all CMDL halon data (a) H-1301 (b) H-1211. Circles represent analyses with the old EC-GC, triangles represent analyses with the new EC-GC, squares are for data obtained by GC-MS (H-1211 only).

drift within this range. Data from the GC-MS and EC-GC systems agree within ±0.1 ppt overall.

One indicator of potential sampling error or storage effects is a comparison of agreement for flask pairs versus that for individual measurements of the same flask. From purely statistical considerations, one would expect flask-pair agreement to be better than the precision for individual measurements if there is no flask or sampling effect. This is because the value obtained for each flask is a mean and, consequently, a closer estimate of the true mean than is an individual measurement. From EC-GC measurements, it is clear that agreement for H-1301 within pairs of simultaneously collected flasks is similar to the analytical precision for repeat measurement of individual flasks (Figure 5.7*a*). Because surface effects in all flasks are not expected to be identical, this indicates that there is little chance of storage having affected H-1301. The median standard deviations for replicate analyses and for flask-pair agreement are both around ±0.01 ppt (±0.5%). However, for H-1211, agreement between flasks is somewhat poorer than for replicate analyses (Figure 5.7*b*). The median standard deviation for replicate analyses is ±0.02 ppt (±0.7%), but for flask pairs is ±0.04 ppt (±1.3%). This is not a large effect and it may be symptomatic of some problem occurring within a flask after it has been sampled.

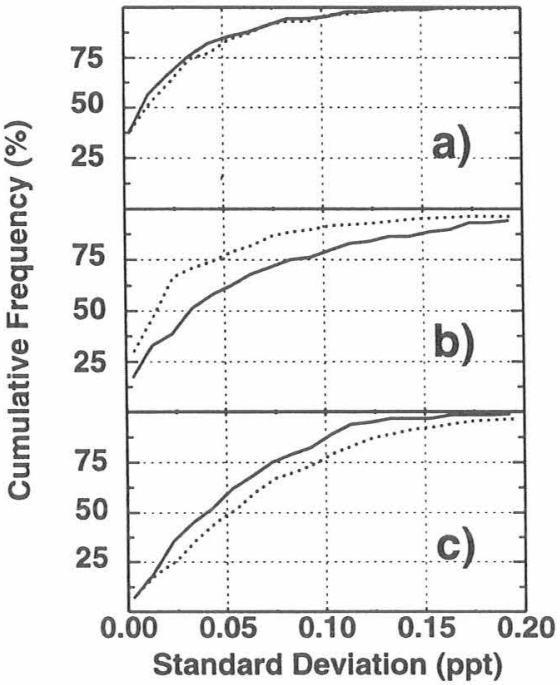

Fig. 5.7. Cumulative error plots for repeat analysis of individual flasks (dotted line) and analysis of flask pairs (solid line): (a) H-1301 by EC-GC, (b) H-1211 by EC-GC, (c) H-1211 by GC-MS.

Whether this effect involves H-1211 directly or some other compound affecting the analysis is uncertain at this time. It does not appear related to sampling site, sampling dates, or time between sampling and analysis. The possibility that it may be something other than H-1211 is underscored by a similar evaluation for GC-MS data. In this case, the agreement for H-1211 between flasks is actually slightly better than that for replicate analyses, as one would expect from purely statistical considerations (Figure 5.7*c*). Because the GC-MS is specific for the m/z = +85 ion from H-1211 and the ECD is less specific, it is more probable that the larger differences between flask pairs, as observed by EC-GC, may be some matrix effect, such as that caused by a co-eluting compound. It is also possible, however, that the effect is just beyond the detection ability of the GC-MS.

5.1.4. Alternative Halocarbon Measurements

Hydrochlorofluorocarbons (HCFCs) are important substitutes for CFCs in industrial applications. Their use will significantly shorten the time required for complete elimination of CFCs in industry [*UNEP*, 1991]. Although HCFCs contain chlorine, models indicate that they have a much reduced potential to deplete stratospheric ozone compared with CFCs. Ozone destruction capacity for HCFCs, as predicted by semi-empirical steady state ozone depletion potentials, ranges between 1 and 12% that of CFC-11 [*WMO*, 1991; *Solomon et al.*, 1992]. However, the ozone depletion potential for HCFCs over short periods, such as the next 5-10 years when chlorine is expected to reach a maximum in the stratosphere, is more accurately estimated with time-dependent ozone depletion potentials [*Solomon and Albritton*, 1992]. Because HCFCs have shorter atmospheric lifetimes than CFC-11, time-dependent depletion potentials can be as much as five times higher than steady-state ozone depletion potentials. For these reasons, and because of uncertainties concerning the chemistry and dynamics of the atmosphere, there is increasing concern over extensive use of HCFCs as replacements for CFCs. Some nations have accelerated the timetable for eliminating HCFCs earlier than recommended by the Copenhagen Amendments to the Montreal Protocol [*UNEP*, 1993]. Monitoring the global spatial and temporal variability of HCFCs is necessary for maintaining an accurate atmospheric chlorine inventory as replacements gain acceptance in the marketplace and for validating model predictions concerning the fate of these compounds in the atmosphere [*Prather and Spivakovsky*, 1990].

Paired sample flasks filled at the four CMDL stations and three cooperative flask sampling locations during 1993 were analyzed in the Boulder laboratory using gas chromatography with mass spectrometric detection for HCFC-22, HCFC-142b, and HCFC-141b [*Montzka et al.*, 1993; 1994*a*, *b*]. Results for both HCFC-22 and HCFC-142b represent a continuation of measurements made in previous years. Before 1993, however, only preliminary mixing ratios were reported for HCFC-142b [*Swanson et al.*, 1993]. In addition to finalizing standardization for HCFC-142b, a consistent set of calibration standards was also prepared for HCFC-141b in 1993.

Chlorodifluoromethane (HCFC-22)

Measurements of the most abundant atmospheric HCFC continued in 1993 (Figure 5.8; Table 5.1). The latitudinally-weighted global mean mixing ratio for HCFC-22 in mid-1993 was 106 ppt (Table 5.2). This is an increase of 4 ppt over the global mean determined for mid-1992 [*Montzka et al.*, 1993]. The growth rate for HCFC-22 from November 1991 through December 1993 is estimated at 4.9 (±1.0) ppt yr^{-1}. The average difference between the northern and southern hemisphere during 1993 was 13 ± 1 ppt.

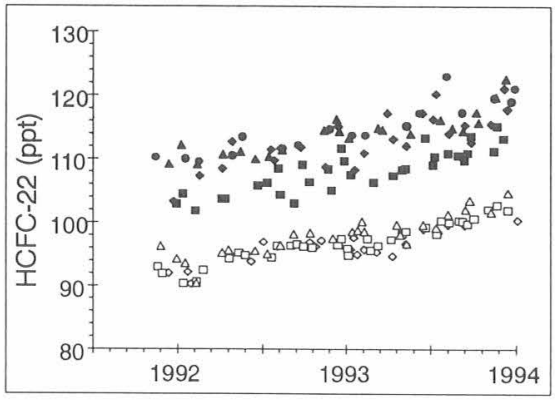

Fig. 5.8. Mixing ratios determined for HCFC-22 from air collected in flasks from seven different remote sampling locations: Alert, (•); BRW, (▲); Niwot Ridge, (♦); MLO, (■); SMO, (Δ); CGO, (□); and SPO, (◊).

1-chloro-1,1-difluoroethane (HCFC-142b)

Hydrochlorofluorocarbon-142b is used predominantly as a substitute for CFC-12 in the fabrication of closed-cell foam [*AFEAS*, 1994]. It was also used to a lesser extent as an aerosol propellant and in refrigeration applications. The shift to HCFC-142b and away from CFC-12 for blowing foam began in 1988, and industry predicted that complete conversion would occur before the end of 1993 [*UNEP*, 1991].

The latitudinally-weighted global mean mixing ratio for HCFC-142b in mid-1993 was 4.3 (±0.1) ppt (Figure 5.9; Table 5.1 and 5.2). This is an increase of 1.0 ppt over the global mean determined for mid-1992. The growth rate for HCFC-142b over the entire sampling period (December 1991 through December 1993) is estimated at 1.1 ppt yr^{-1}.

Mixing ratios determined for HCFC-142b during early 1992 in the northern hemisphere (Figure 5.9) are in reasonable agreement with those reported by *Schauffler et al.* [1993] from air collected in the upper troposphere

TABLE 5.1. CMDL Measurements of HCFCs from Flasks (1991-1993)

Station	Date	HCFC-22 (ppt)	HCFC-142b (ppt)	HCFC-141b (ppt)	Station	Date	HCFC-22 (ppt)	HCFC-142b (ppt)	HCFC-141b (ppt)
ALT	1991.871	110.2			BRW	1993.767	117.4	5.8	1.29
ALT	1992.052	110.0	3.6		BRW	1993.781	115.8	6.0	1.48
ALT	1992.128	109.5	3.8		BRW	1993.882	119.8	5.9	1.86
ALT	1992.328	110.5	4.3		BRW	1993.943	122.6	6.4	1.97
ALT	1992.385	113.4	4.1						
ALT	1992.620	111.5	4.1		CGO	1991.885	93.0		
ALT	1992.713	112.1	4.1		CGO	1991.910	91.9		
ALT	1992.907	114.7	5.0	0.55	CGO	1992.036	90.3	2.3	
ALT	1993.038	113.6	5.0	0.65	CGO	1992.115	90.6	2.4	
ALT	1993.112	113.7	5.4	0.70	CGO	1992.153	92.4	2.6	
ALT	1993.362	115.2	5.5	0.93	CGO	1992.306	94.2	2.2	
ALT	1993.438	117.2	5.7	0.87	CGO	1992.363	95.1	2.7	
ALT	1993.595	122.9		1.05	CGO	1992.402	94.8		
ALT	1993.688	117.2	5.6	1.51	CGO	1992.555	94.5	2.6	
ALT	1993.880	119.5	6.4	1.64	CGO	1992.587	96.2	2.7	
ALT	1993.975	119.0	6.8	1.99	CGO	1992.669	96.3	2.2	
ALT	1993.995	121.0	7.6	1.87	CGO	1992.705	96.6	2.4	
					CGO	1992.746	96.2	3.0	
BRW	1991.951	109.2			CGO	1992.798	96.0	2.9	
BRW	1992.022	112.2			CGO	1992.951	96.4*	3.3	0.23
BRW	1992.120	109.1	3.3		CGO	1992.970	97.4*	2.7	0.19
BRW	1992.268	110.7	3.8		CGO	1993.008	95.8	3.0	0.24
BRW	1992.372	111.2	3.3		CGO	1993.014	94.8	3.7	0.20
BRW	1992.459	110.0	4.1		CGO	1993.126	97.4	2.9	0.20
BRW	1992.538	110.4	3.5		CGO	1993.145	95.6	3.6	0.14
BRW	1992.618	111.4	4.2		CGO	1993.186	96.3	3.1	0.26
BRW	1992.866	114.5	4.8		CGO	1993.266	97.3	3.3	0.35
BRW	1992.940	116.3	5.3		CGO	1993.334	98.2	3.6	0.33
BRW	1992.959	114.3*	4.9	0.55	CGO	1993.356	98.6	3.4	0.35
BRW	1993.016	113.2	5.1	0.58	CGO	1993.471	99.2	3.7	0.34
BRW	1993.186	114.9	5.5	0.69	CGO	1993.537	98.2	3.6	0.34
BRW	1993.214	114.6	4.5	0.91	CGO	1993.564	100.3	4.0	0.43
BRW	1993.381	114.0	5.1	0.85	CGO	1993.608	99.9	3.7	0.46
BRW	1993.556	116.2	5.0	1.04	CGO	1993.669	100.2	3.3	0.45
BRW	1993.627	114.9	5.7	1.24	CGO	1993.688	100.2	3.5	0.45
BRW	1993.688	114.5	5.3	1.34	CGO	1993.718	99.8	3.8	0.42

TABLE 5.1. CMDL Measurements of HCFCs from Flasks (1991-1993)—Continued

Station	Date	HCFC-22 (ppt)	HCFC-142b (ppt)	HCFC-141b (ppt)	Station	Date	HCFC-22 (ppt)	HCFC-142b (ppt)	HCFC-141b (ppt)
CGO	1993.756	100.6	3.5	0.53	NWR	1993.606	114.1	5.2	1.35
CGO	1993.841	102.0	4.2	0.45	NWR	1993.701	115.4	5.5	1.63
CGO	1993.890	102.7	3.9	0.52	NWR	1993.740	112.6	5.3	1.29
CGO	1993.953	101.9	4.1	0.59	NWR	1993.855	115.5	5.9	1.69
					NWR	1993.932	121.1	6.1	1.98
MLO	1991.995	102.9			NWR	1993.951	117.8	5.9	1.88
MLO	1992.033	104.4	2.9						
MLO	1992.109	101.8	3.1		SMO	1991.901	96.2		
MLO	1992.262	103.6	2.9		SMO	1991.995	94.2		
MLO	1992.281	103.6	3.2		SMO	1992.046	93.6	2.4	
MLO	1992.473	105.7	3.5		SMO	1992.112	90.4	2.4	
MLO	1992.530	106.1	3.6		SMO	1992.262	95.2	2.5	
MLO	1992.596	108.5	3.3		SMO	1992.301	95.7	2.9	
MLO	1992.607	104.3	3.0		SMO	1992.456	95.5	2.8	
MLO	1992.691	103.0	3.3		SMO	1992.530	95.0	2.7	
MLO	1992.740	109.1	5.0		SMO	1992.607	96.3	3.3	
MLO	1992.779	106.3	3.9		SMO	1992.686	98.2	2.9	
MLO	1992.893	108.4	4.0		SMO	1992.784	98.3	3.8	
MLO	1992.913	105.0	3.6		SMO	1992.921	97.5		
MLO	1992.970	111.6	4.6		SMO	1993.036	98.6	2.6	0.25
MLO	1992.989	109.7*	4.6	0.41	SMO	1993.069	98.8	2.9	0.28
MLO	1993.027	107.5	3.8	0.41	SMO	1993.093	100.2	3.3	0.40
MLO	1993.162	106.3	3.9	0.53	SMO	1993.107	98.6	3.6	0.29
MLO	1993.280	107.4	4.2	0.66	SMO	1993.299	99.6	3.4	0.39
MLO	1993.334	108.2	4.8	0.71	SMO	1993.321	98.1	3.7	0.32
MLO	1993.353	108.4	4.2	0.70	SMO	1993.359	96.7	3.3	0.33
MLO	1993.469	113.3	4.9	0.91	SMO	1993.455	99.6	3.6	0.46
MLO	1993.515	109.1	4.5	0.87	SMO	1993.532	99.2	3.4	0.36
MLO	1993.526	110.4	4.8	0.71	SMO	1993.603	101.3	3.9	0.50
MLO	1993.603	110.9	5.6	1.02	SMO	1993.704	102.0	4.0	0.61
MLO	1993.660	110.6	4.9	1.17	SMO	1993.729	103.5	3.7	0.61
MLO	1993.699	109.8	4.7	1.13	SMO	1993.855	101.7	3.8	0.63
MLO	1993.718	111.0	4.8	1.20	SMO	1993.953	104.7	4.4	
MLO	1993.737	113.6	5.1	1.10					
MLO	1993.871	111.3	4.7	1.43	SPO	1991.948	92	2.1	
MLO	1993.890	115.2	5.3	1.39	SPO	1992.063	92.1	2.1	
MLO	1993.929	113.2	5.1	1.39	SPO	1992.079	90.3	2.1	
					SPO	1992.434	93.8	3.1	
NWR	1991.978	103.3			SPO	1992.506	96.9	2.7	
NWR	1992.131	107.3	3.5		SPO	1992.590	96.2	2.8	
NWR	1992.265	108.4	3.4		SPO	1992.694	96.4	2.8	
NWR	1992.322	112.7	3.5		SPO	1992.781	96.8	2.7	
NWR	1992.552	111.5	4.0		SPO	1992.817	96.2	2.5	
NWR	1992.571	109.7	3.9		SPO	1992.853	97.1	3.0	
NWR	1992.609	111.7	3.6		SPO	1993.022	95.7	3.0	0.24
NWR	1992.727	111.8	4.0		SPO	1993.044	97.6	3.1	0.25
NWR	1992.877	108.7	3.6		SPO	1993.066	94.9	2.9	0.28
NWR	1992.954	115.1	4.5	0.57	SPO	1993.104	95.7	3.6	0.20
NWR	1993.049	108.3	5.8	0.47	SPO	1993.181	95.4	2.9	
NWR	1993.104	110.9	4.4	0.69	SPO	1993.274	94.7	2.7	
NWR	1993.244	117.2	6.0	1.00	SPO	1993.353	96.6	3.3	0.36
NWR	1993.280	113.1	4.6	0.84	SPO	1993.458	98.9	3.2	0.30
NWR	1993.356	112.1	4.9	0.89	SPO	1993.545	98.4	3.5	0.38
NWR	1993.452	117.2	5.3	1.08	SPO	1993.603	99.7	3.0	0.37
NWR	1993.515	116.3	5.3	1.33	SPO	1993.701	99.6	3.6	0.31
NWR	1993.529	120.3	5.7						

*Revised from that reported in *Swanson et al.* [1993]

TABLE 5.2. Estimates for Mid-Year Global Mean Mixing Ratios and Globally-Averaged Growth Rates

	1992 Mixing Ratios (ppt)	1993 Mixing Ratios(ppt)	All Data Growth Rates
HCFC-22	102	106	4.9 ppt yr^{-1}
HCFC-142b	3.3	4.3	1.1 ppt yr^{-1}
HCFC-141b	—	0.7	>100% yr^{-1}

of the northern hemisphere (2.9-3.9 ppt, CMDL versus 2.1-3.4 ppt, NCAR) [*Montzka et al.*, 1994*a*]. Informal comparisons of gas standards prepared independently at these two laboratories were performed at CMDL and indicate that the standards agree to within 5%.

When compared with levels calculated from emission estimates [*AFEAS*, 1994] and a finite-increment model, the results from both laboratories are 1.5-1.8 times (or 1.3-1.5 ppt) greater than expected [*Montzka et al.*, 1994*a*]. Although the reasons for this discrepancy are unclear at present, it is not likely that this difference results from inaccurate estimates of atmospheric lifetime for HCFC-142b. HCFC-142b has been emitted into the atmosphere for only a short period of time relative to its predicted atmospheric lifetime and, therefore, model calculations performed with a much longer lifetime than 20 years (100-1000 years) do not remove the discrepancy between observations and model results based on available emission estimates.

1,1-dichloro-1-fluoroethane (HCFC-141b)

HCFC-141b is currently used as a CFC-11 substitute for blowing closed-cell foams and as a substitute for CFC-113 as a solvent and cleansing agent. Unlike HCFC-142b, HCFC-141b was not commercially available until the beginning of 1993 when toxicological studies were scheduled to be completed [*UNEP*, 1991]. Before 1993, many companies in the foam sector stated their intention to eliminate CFC-11 for this use during that year [*UNEP*, 1993; *EPA*, 1993]. While substitution of CFC-113 with HCFC-141b is also likely to occur rapidly, industry experts estimate that only ~5% of past demand for CFC-113 will be satisfied with HCFCs owing to the many alternative processes and approaches that were developed by industry to reduce the amount of CFC-113 needed in these applications [*UNEP*, 1991].

The latitudinally-weighted global mean mixing ratio for HCFC-141b in mid-1993 was 0.7 (±0.1) ppt (Figure 5.10; Table 5.1 and 5.2) [*Montzka et al.*, 1994*a*]. The global mean mixing ratio increased exponentially during 1993, at greater than 100% yr^{-1}. The rapid increase in ambient mixing ratio during 1993 is likely the result of a dramatic shift towards use of HCFC-141b in industrial applications after toxicological studies were completed.

Recently, *Schauffler et al.* [1995] reported mixing ratios for HCFC-141b from samples collected during a number of cruises in the Pacific, Southern, and Arctic Oceans over the past 2 years. A comparison of mixing ratios determined from samples collected at similar times and at similar latitudes, reveals that results from the two independent laboratories agree to within 0.1 ppt [*Schauffler et al.*, 1995].

Stability of HCFCs in Flasks

Because measurements are based on the analysis of air contained within flasks that were filled at an earlier date, it is necessary to ensure that these compounds are stable within these containers over time before reliable and accurate mixing ratios can be reported. The potential for production and/or loss of HCFC-22, -142b, and -141b within sample flasks is investigated here by: (1) reanalyzing air within a flask after a period of time

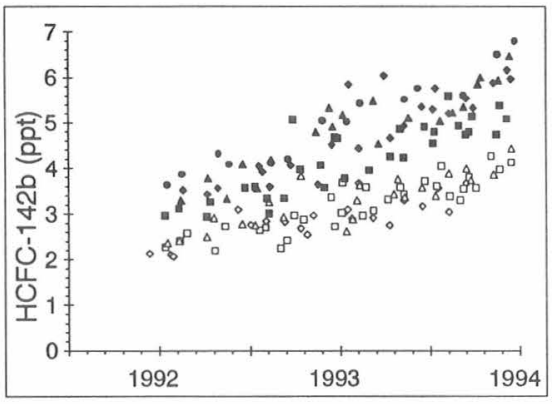

Fig. 5.9. Mixing ratios determined for HCFC-142b from air collected in flasks from seven different remote sampling locations: Alert, (•); BRW, (▲); Niwot Ridge, (♦); MLO, (■); SMO, (Δ); CGO, (□); and SPO, (◊).

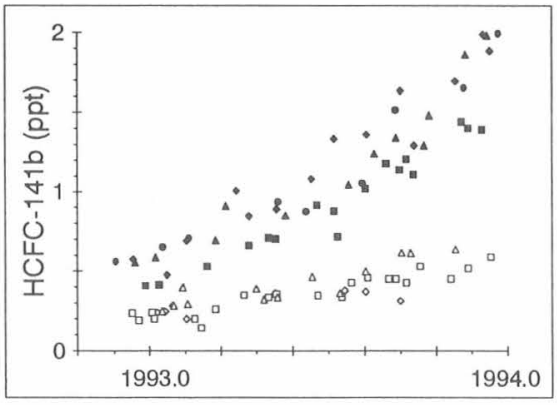

Fig. 5.10. Mixing ratios determined for HCFC-141b from air collected in flasks from seven different remote sampling locations: Alert, (•); BRW, (Δ); Niwot Ridge, (♦); MLO, (■); SMO, (Δ); CGO, (□); and SPO, (◊).

has elapsed to see if consistent results are obtained; (2) determining if relationships between the amount of time the air is stored in a flask and reported mixing ratios are apparent; (3) determining if differences attributable to humidity levels within a flask are apparent in results from SPO and CGO; and (4) determining if disagreements in HCFC mixing ratios within simultaneously filled flasks are significant relative to the precision of the analysis.

After they were received in Boulder, selected flasks were analyzed two or more times to study the effects of storage time on different compounds within flasks (Figure 5.11). Results from the two analyses are compared with the variability observed for duplicate injections of air from flasks that were collected in 1992 and 1993. For more than 90% of the flasks that were reanalyzed, the results obtained for all three HCFCs were within the 95% confidence interval for variability observed for duplicate injections of air from flasks. The larger differences observed for HCFC-141b and -142b upon reanalysis are associated with the initial stages of the measurement program when mixing ratios and signal-to-noise ratios were exceptionally low.

Although the second analysis was usually performed under identical instrumental conditions, a more polar, chromatographic column was sometimes used (Figure 5.11). In the chromatographic analysis of complex environmental samples, it is useful to compare results obtained under different instrumental conditions to ensure that these results are independent of the conditions chosen. Analysis of air samples with capillary columns having different polarity allows for an estimate of the importance of coeluting compounds on the results obtained for atmospheric HCFCs using this chromatographic instrument. For all three HCFCs, results obtained during reanalysis with the more polar column were not significantly different from the initial analysis. Because it is unlikely that a compound would interfere consistently under different instrumental conditions, these results suggest that measurements of these HCFCs are free of these types of interferences.

Flask samples sent from the stations in 1991, 1992, and 1993 (excluding SPO) were analyzed at the CMDL Boulder laboratories anywhere from 2 to 76 days after they were collected (mean = 24 days; median = 22 days). These delays result from shipping and instrument availability. Longer delays are associated with samples collected at SPO because no shipments leave this site during the southern hemisphere winter. To ascertain if these delays adversely affect HCFC measurements, residuals from loess fits to the data obtained at each station are compared with the time elapsed between sampling and analysis of each flask (Figure 5.12). A loess smoothing fraction of 0.3 was used to generate the residuals plotted in this figure to remove variability associated with seasonality and non-linear growth rates but retain short-term variability. No

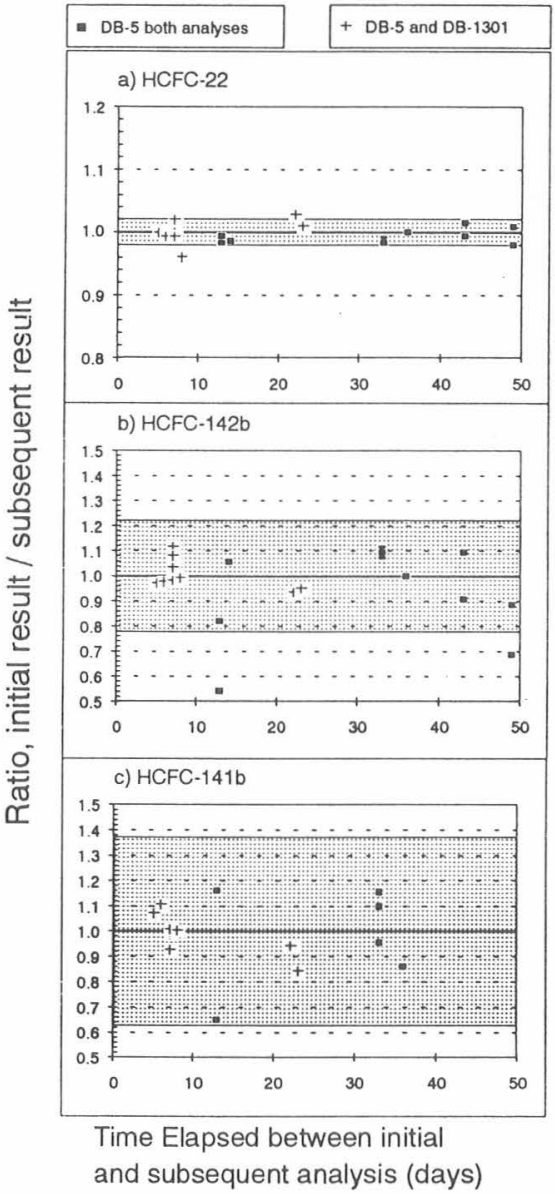

Fig. 5.11. Results obtained when air within samples flasks was re-analyzed after a period of time had elapsed for (*a*) HCFC-22, (*b*) HCFC-142b, and (*c*) HCFC-141b. Squares represent re-analyses that were performed under identical instrumental conditions. Plus symbols (+) represent results from re-analyses that were performed with a more polar analytical column (DB-1301 versus DB-5). The shaded area represents 2 times 95% of the range of variability observed for duplicate injections of air from all flasks collected in 1992 and 1993.

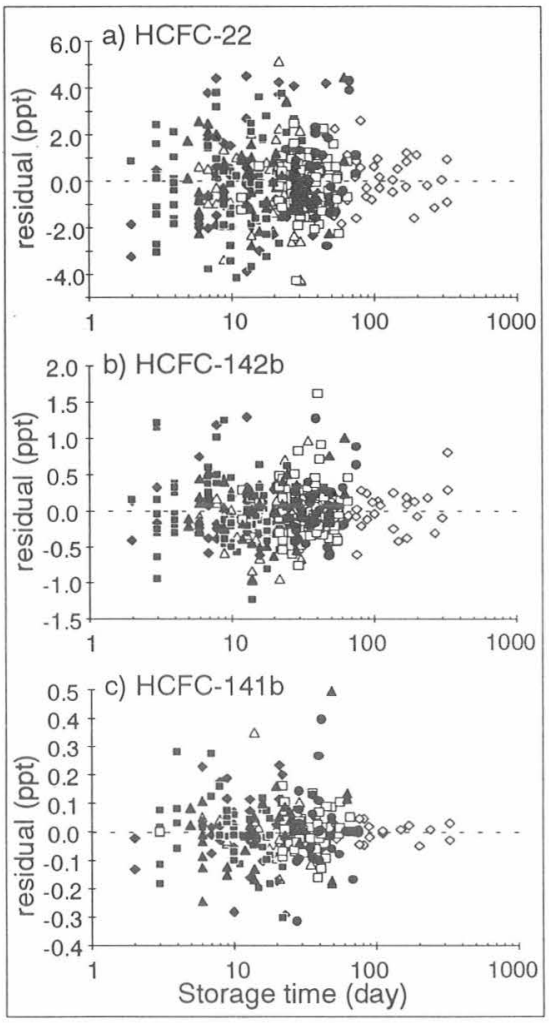

Fig. 5.12. Residuals from loess fits to flask data obtained over time are plotted against elapsed time between flask collection and analysis for (*a*) HCFC-22, (*b*) HCFC-142b, and (*c*) HCFC-141b. Symbols represent the different sampling stations (see Figure 5.8). The loess fits are performed for each compound at each sampling station with a smoothing fraction of 0.3.

significant relationship between storage time and residual is observed, and scatter in the residual does not increase at longer storage times. Although the scatter observed in Figure 5.12 represents an upper limit for the magnitude of problems associated with sample storage in these flasks under a wide range of sample humidities, it also encompasses variability associated with the atmosphere and instrumental analysis.

The effect of humidity on mixing ratios for HCFCs within flasks can be investigated by comparing data from SPO with the results obtained at CGO. For compounds emitted predominantly in the northern hemisphere, and for which atmospheric growth and loss rates are small when compared with intrahemispheric mixing rates, similar mixing ratios are observed at SPO and CGO [*Steele et al.*, 1987; *Elkins et al.*, 1993]. Ambient conditions at these two locations, however, are significantly different; while air collected at SPO can be extremely dry, air is sampled from within the marine boundary layer at CGO and ambient temperatures are, on average, ~60°C higher. Losses of certain compounds such as CCl_4 within electropolished stainless-steel flasks are known to be dependent upon the amount of water in a flask [*Schauffler et al.*, 1993; *Montzka et al.*, 1994*b*]. Despite large losses of CCl_4 within a number of flasks filled at SPO, ambient mixing ratios for HCFC-22 and HCFC-142b are very similar at both of these stations (Figure 5.13). These results suggest that within the range of humidities encountered at these two stations, mixing ratios determined for these HCFCs are independent of the amount of water present within these flasks [*Montzka et al.*, 1994*b*].

Based on the majority of measurements made for HCFC-141b in flasks collected at SPO, a similar conclusion can be drawn for this HCFC. However, in three flasks it appears as if mixing ratios from SPO are low relative to the measurements made concurrently at CGO. While this suggests that HCFC-141b may undergo losses within extremely dry flasks, rather large uncertainties are associated with these measurements owing to the extremely low mixing ratios of this compound in the southern hemisphere during early 1993. Furthermore, observed differences between mixing ratios determined for HCFC-141b within flasks collected at SPO and CGO are not correlated with carbon tetrachloride losses in these flasks, suggesting that the characteristics of a flask that cause losses of carbon tetrachloride do not affect mixing ratios determined for HCFC-141b.

Results from the flask measurement program are based on flask pairs collected simultaneously and in a parallel flow arrangement. During analysis, each flask is treated independently, and the results obtained are averaged to arrive at a best estimate for ambient air mixing ratios at the time the flask was filled. Results obtained for compounds within simultaneously filled flasks should agree to within the analytical precision of the instrument. Disagreements between mixing ratios determined within flasks that are filled in parallel can indicate problems associated with filling flasks, flask cleanliness, and compound integrity within flasks.

For all three HCFCs, the median difference observed between simultaneously filled flasks is similar to the median uncertainty associated with repetitive injections of air from a single flask (Figure 5.14). Furthermore, the entire distribution of flask-pair differences are

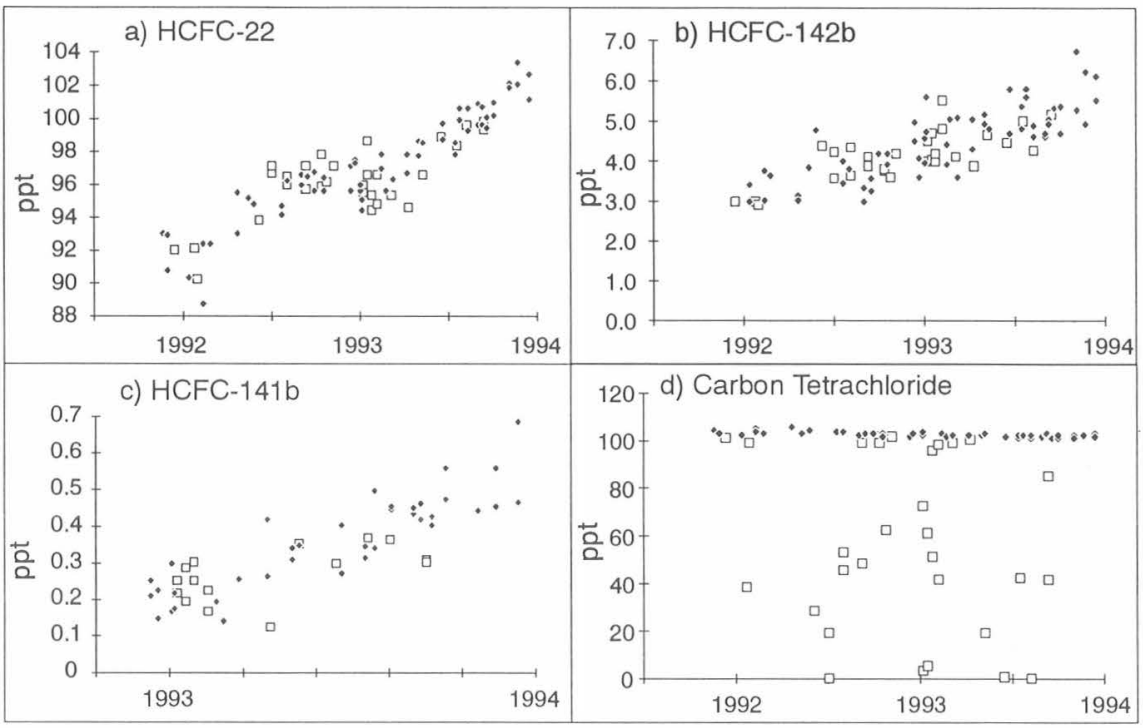

Fig. 5.13. Mixing ratios observed within individual flasks for different HCFCs at both CGO (♦) and SPO (□) for (*a*) HCFC-22, (*b*) HCFC-142b, (*c*) HCFC-141b, and (*d*) CCl_4.

similar to, if not lower than, observed analysis standard deviations for all three HCFCs, and this suggests that no measurable differences are observed in flasks filled simultaneously at the sampling stations. For HCFC-22, however, there are instances where values obtained from simultaneously filled flasks disagree significantly (≤5% occurrence for disagreements greater than 3 ppt). Sample pairs with such large differences are not used when calculating atmospheric growth rates or global background mixing ratios [*Montzka et al.*, 1993]. In the discussion above, it was concluded that HCFC-22 is stable within flask canisters for extended periods under widely differing ambient water mixing ratios and, therefore, it is difficult to explain these larger differences based on the instability of HCFC-22 within flasks. A more likely cause for these larger differences rests with problems associated with filling flasks or flask cleanliness. Separate analyses have shown that levels of HCFC-22 are typically 100-1000 times higher in laboratory air than in ambient air at remote sampling locations (S. Montzka, unpublished data). Occasional problems with small leaks or insufficient purging of flasks either during filling or analysis could generate the type of result observed.

Measurement of Additional Chlorinated Compounds with GC-MS Instrumentation

The versatility of the GC-MS technique allows for the detection of many different compounds within a single chromatogram. In addition to the compounds already quantified with GC-MS during a single analysis of air from flasks (HCFCs, CFCs, halons, methyl halides, methyl chloroform, and carbon tetrachloride), monitoring of several more chlorinated compounds began in 1993. Mixing ratios for methyl chloride (CH_3Cl), dichloromethane (CH_2Cl_2), chloroform ($CHCl_3$), and tetrachloroethylene (C_2Cl_4) were determined for air contained within flasks. Measurements of these additional compounds are performed by monitoring ions unique to these chlorinated hydrocarbons at predetermined elution times. No additional changes to the experimental technique are required. Preliminary results for these compounds are presented in Figure 5.15.

5.1.5. Gravimetric Standards

New Blending Manifold

An ultraclean gas blending manifold was designed and built for the preparation of gravimetric standards.

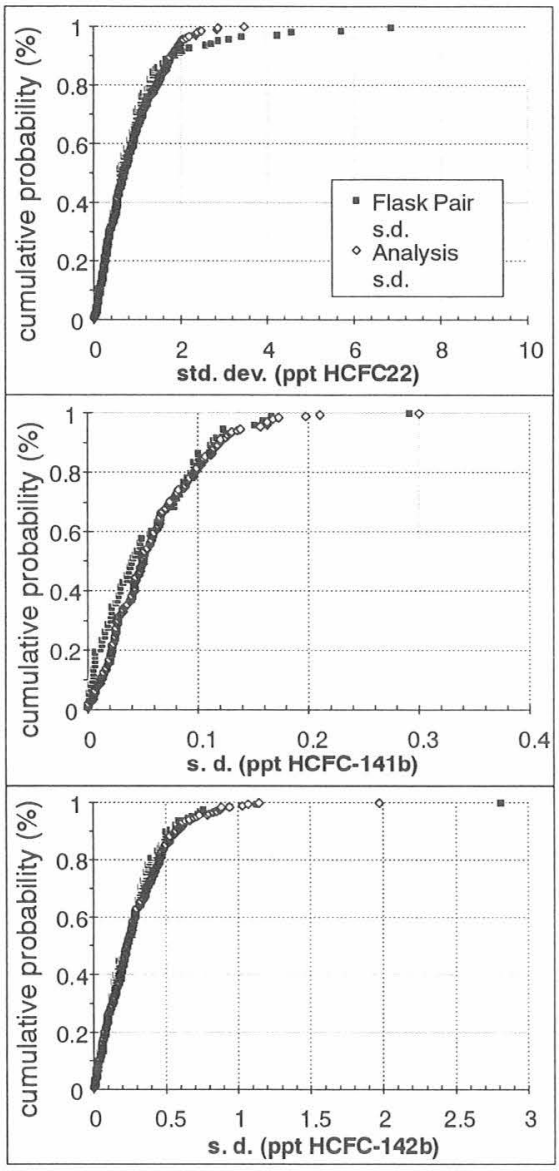

Fig. 5.14. Standard deviations obtained for duplicate injections of air from individual flasks (analysis s.d.) plotted on a cumulative probability scale. Also shown are the differences measured in simultaneously filled flasks (pair standard deviations). The data presented are for all samples collected and analyzed through the end of 1993.

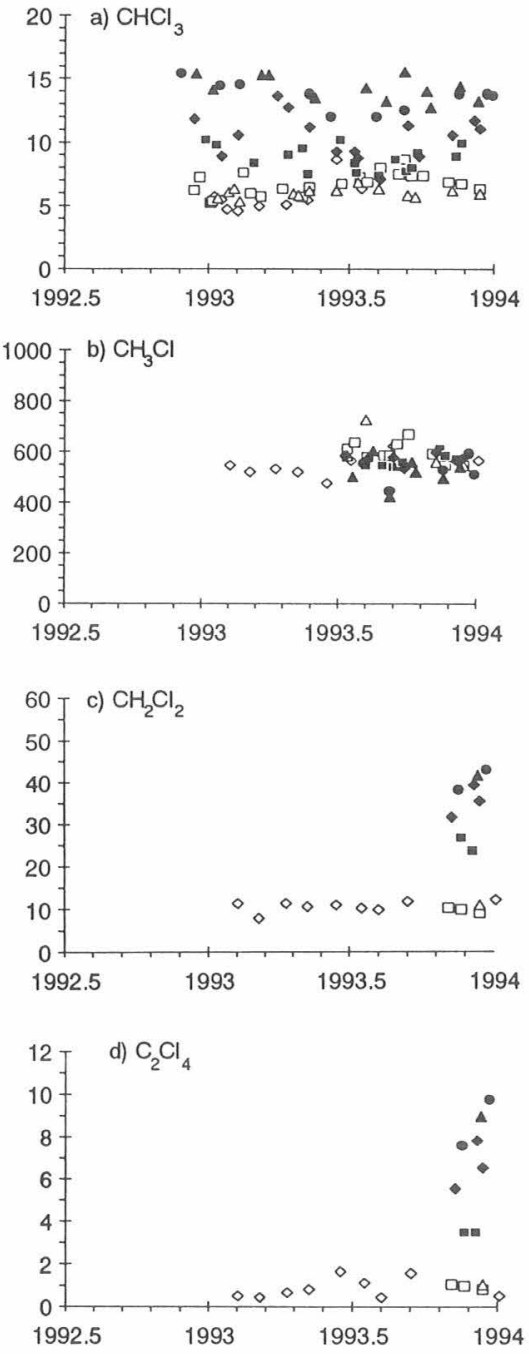

Fig. 5.15. Mixing ratios determined for different chlorinated compounds from air collected in flasks at seven different remote sampling stations. Symbols are identical to those in Figure 5.8. Mixing ratios for compounds other than CH_3Cl are reported relative to a preliminary calibration scale.

The main manifold system (Figure 5.16) was made using electropolished stainless steel tubing (6.35 mm o.d.) that was connected together using an automatic tube welder providing relatively smooth weld joints on

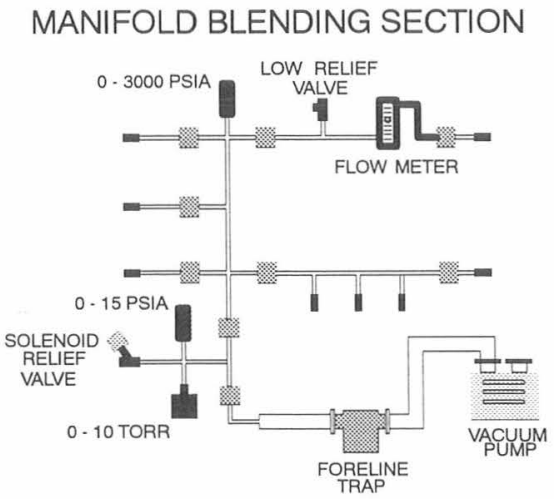

Fig. 5.16. Main section of gas blending manifold.

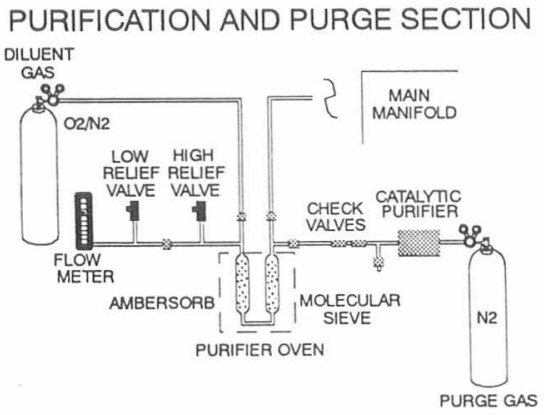

Fig. 5.17. Purification section of gas blending manifold.

the interior surface of the tubing. Welded, metal-gasket face-seal fittings were also used to connect the subsections of the manifold together and at the cylinder connection ports. Packless all-metal diaphragm valves with welded, metal-gasket face-seal fittings were used at all valve locations. Three strain gauges were installed on the manifold system for pressure measurements. A 0-20.7 MPa gauge is used for measuring pressure in the main part of the manifold. Two additional gauges measure pressures from vacuum to 103.4 kPa and from vacuum to 1.33 kPa. These low pressure gauges are isolated from the main part of the manifold by a valve in the vacuum segment of the manifold. The low pressure gauges are protected from high pressures by using a high-vacuum solenoid valve wired to a pressure-readout meter. Vacuum is achieved using a high flow rate vacuum pump. A foreline trap containing molecular sieve prevents oil vapors from entering the manifold. The manifold can be evacuated to approximately 4 Pa. A gas purification section of the manifold (Figure 5.17) is used for further purification of diluent gases such as air or N_2 supplied by commercial gas suppliers. Two traps containing Ambersorb and Molecular Sieve 13X can be heated to 250°C while they are purged with high-purity N_2. The traps are then cooled to room temperature prior to use. The N_2 used to purge the traps can also be used to purge the manifold of residual gases.

Standards

A suite of calibration standards containing N_2O and CO_2 in air were prepared this year for the CSIRO Division of Atmospheric Research. The standards were gravimetrically prepared at nominal mixing ratios ranging from 265 ppb to 345 ppb of N_2O. Carbon dioxide was added to the parent N_2O mixture that was used to prepare the ppb level N_2O mixtures at nominal mixing ratios ranging from 330 ppm to 430 ppm.

Standards containing methyl bromide (CH_3Br) and methyl chloride (CH_3Cl) in air were prepared this year. In the past, both methyl halides were used as refrigerants, solvents, and in organic synthesis [*Braker and Mossman*, 1980]. Methyl bromide is mostly used as a pesticide. Small aliquots of each compound were added to individual Aculife-treated aluminum compressed-gas cylinders providing ppb level mixtures. The Aculife treatment provides an internally inert surface that prevents both methyl halides from reacting with the aluminum. The mixtures were then blended together into one cylinder. Gravimetric standards containing from 5 to 25 ppt of CH_3Br and 400 to 1000 ppt of CH_3Cl were then prepared. The response factors (GC-MS response per mole injected) for both ppb and ppt level CH_3Br and CH_3Cl standards were consistent to within 5%.

Standards containing HCFC-141b and HCFC-142b were also prepared using the same gravimetric techniques used to prepare the methyl halide standards. Single component standards containing each HCFC were prepared at ppb levels. The standards at ppb levels were combined together, and the mixture containing both compounds was used to prepare standards at 5, 25, 50, and 500 ppt with a ratio of approximately 1:1 for HCFC-141b and HCFC-142b. Response factors determined by GC-MS analysis of each HCFC within the suite of standards (ppt to ppb levels) were consistent to within 5%.

5.2. Special Projects

5.2.1. Aircraft Project: Stratospheric Photochemistry, Aerosols, and Dynamics Expedition (SPADE)

Compact correlations between long-lived tracer molecules (e.g., CFCs, N_2O, CH_4, and H_2O) in the

stratosphere are used to calculate the average age of air samples [*Pollock et al.*, 1992], the chlorine budget of the atmosphere [*Kawa et al.*, 1992; *Woodbridge et al.*, 1995], the ozone depletion potentials of substitute CFCs [*Pollock et al.*, 1992], and lifetimes of long-lived trace gases [*Plumb and Ko*, 1992]. The results of tracer correlations of CFC-11, CFC-113, CH_4, and N_2O in the midlatitudes during SPADE in November 1992 and through April and May 1993, are compared to an earlier mission, the Airborne Arctic Stratospheric Expedition (AASE-II), from August 1991 through March 1992. Trace gases whose local lifetime are longer than quasi-horizontal transport time are in climatological slope equilibrium. A scatter plot of the mixing ratio of one versus the other collapses to a compact curve because they share surfaces of constant mixing ratio [*Plumb and Ko*, 1992]. In general, the long-lived tracers such as N_2O, CH_4, CFC-11, and CFC-113 reach slope equilibrium throughout the stratosphere, hence define a compact correlation when plotted against each other.

Exceptions to this general rule can occur when mixing across exchange surfaces is faster than diffusion along mixing ratio isopleths. One such exception occurred in Stratospheric Photochemistry Dynamics and Aerosols Expedition (SPADE) during the flight of May 7, 1993. Using the tracer correlations during slope equilibrium allows the calculation of lifetimes of the tracers in the stratosphere, and in some cases in the absence of tropospheric sinks, the total atmospheric lifetime of the specie.

For the first time, CH_4 measurements from an in situ GC are compared against an in situ tunable diode laser (TDL) spectrometer and three different water vapor techniques conducted during SPADE.

Experimental Methods

The Airborne Chromatograph for Atmospheric Trace Species (ACATS), was a cooperative development between CMDL and the NOAA Aeronomy Laboratory (AL). The first ACATS instrument was a single-channel GC capable of measuring CFC-11 and CFC-113 once every 120 seconds aboard the NASA ER-2 aircraft during AASE-II. The instrument remained unchanged in the November 1992 deployment of SPADE. A second GC channel was added for CH_4 measurements during the second deployment of SPADE in April and May 1993. Because of longer times required for separation of CH_4 and CO from the air peak, both channels sampled every 180 seconds. ACATS occupies a rectangular space (45.7 cm wide × 86.4 cm long × 20.3 cm tall) inside the AL reactive nitrogen package and mounted together inside the equipment bay (Q-bay) of the ER-2 aircraft. The two instruments shared gases on a common cylinder rack, pump motor, and data acquisition system to reduce space and weight. The GC's sample air inlet, forward facing, L-shaped, stainless steel tubing, 6.4 mm diameter was located on the lower Q-bay hatch extending 20 cm away from the fuselage in order to sample outside the aircraft (Figure 5.18).

Typical ER-2 flight speeds of 200 m s^{-1} (0.8 mach) required faster sampling rates than commercial GCs provide to gain adequate data spacial resolution. The sampling rates are made possible by a 12-port, 2-position gas sample valve from Valco Instruments, Inc. (Houston, Texas). The gas sample valve diverts or heart-cuts the large oxygen peak away from the ECD to improve the resolution of the smaller trace species. In addition to the gas sample valve, each channel contains two gas chromatographic separation columns, a pre-column and a main column, and an ECD from Shimadzu Corp. (Tokyo, Japan). Upon injection of the sample into the GC, the gas sample valve position is switched and the carrier gas sweeps the sample 5 cm^3 for CFC channel and 15 cm^3 for CH_4 channel into the pre-column and subsequently through the main analytical separation column. Both channels share a clean supply of ultra-high purity N_2 carrier gas

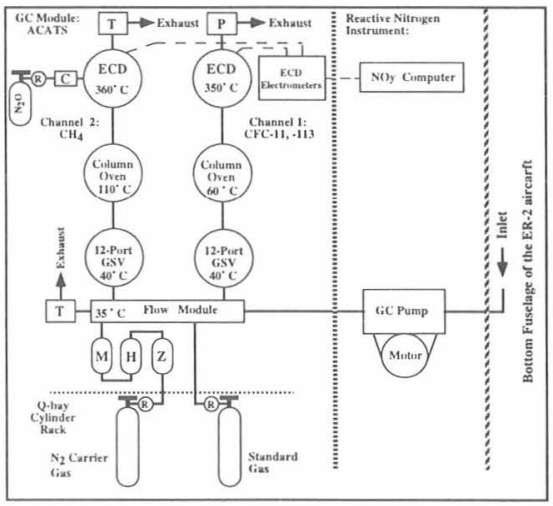

Fig. 5.18. Schematic of the ACATS. The instrument contained two separate GC channels that were used to measure CFC-11, CFC-113, and CH_4 with 180-seconds resolution. The nitrogen carrier gas was scrubbed in series through a hot zirconium (labeled Z) column (9.5 cc at 350°C) to remove CFCs, a Hopcalite (H) trap (manganese dioxide and copper oxide mixture, 40 cc at ambient temperature) to oxidize possible CO contamination of CO_2, and finally a molecular sieve (M) 13X trap (40 cc at ambient temperature). The crimped (C) tubing located after the regulator (R) of the pure (N_2O tank that delivers 20 ppm of N_2O into the ECD of channel 2. A proportional-integral-differential (PID, MKS Instruments, Massachusetts) controller (P) maintain the pressure to about 93.0 ± 0.1 kPa on the ECD of channel 1, while two pressure relief valves (T. Tavco, California) maintain separately the ECD pressure of channel 2 and the pressure of the sample loop to about 93.0 ± 0.1 kPa.

(99.999%, General Air, Colorado) and a stream selection array of solenoids that can supply either sample air or calibration gas while maintaining continuous flow throughout the flight.

The measurement technique for CH_4 was adapted from the work of *Goldan et. al.* [1982]. The advantage of this technique is that a flame, a problem for some high-altitude applications, is not required as in the flame ionization detector for detection of CH_4. An ECD can be "sensitized" to CH_4 and CO by doping the carrier gas into the detector with mixing ratios about 15-50 ppm of nitrous oxide. Pure N_2O was delivered to the CH_4 ECD through a small piece of crimped tubing into the ECD make-up flow of ~10^{-3} cm^3 min^{-1}, yielding a mixing ratio of approximately 20 ppm of N_2O in N_2 inside the ECD.

The halocarbon channel used a 1 m pre-column and a 2 m analytical column of 10% OV-101 (Analabs, Massachusetts) preconditioned at 170°C and temperature controlled at 55°C. During the course of the SPADE mission, two different column packing combinations were used on the CH_4 channel. In the first, a pre-column with a 3.2-mm o.d. and 3-m long was packed with Porapak Q (a porous polymer) was used. It was pre-conditioned at 230°C with 20-30 cm^3 min^{-1} N_2 flow for about 8 hours. The main column of 3.2-mm o.d. by 3-m was packed with molecular sieve, conditioned always to 350°C. Unfortunately, Porapak Q produced CO at temperatures above 50°C. At 100°C, mixing ratios in excess of 500 ppb of CO were found. In the second combination, a pre-column (3.2-mm o.d. by 3-m long) packed with silica gel and was preconditioned at 350°C with 20-30 cm^3 min^{-1} N_2 flow did not produce any detectable CO (>26 ppb). This pre-column was temperature controlled at 50°C with a backflush flow of 100 cm^3 min^{-1} maintained by a differential pressure flow controller (Model VCD-1000, Porter Instruments, Pennsylvania). The main column was increased to 4.8 mm o.d., with a flow controlled at 60 cm^3 min^{-1} by a mass flow controller (Model FC-260, Tylan Corp., California), and a constant temperature of 105°C. To maintain constant detector sensitivity, the ECD housing was purged with a 3 cm^3 min^{-1} flow rate of pure N_2, operated at a constant current of 1 nA, and were pressure controlled at 93 kPa. The temperatures of the ECDs on the halocarbon and CH_4/CO channels were controlled with an Omega (Stamford, Connecticut) temperature controller (Model CN9000A) at 350°C and 360°C, respectively.

Every fifth sample injection was a multi-component standard with 600 ppb of CH_4, 57 ppt of CFC-113, and 130 ppt of CFC-11. This yielded a single-point calibration every 15 minutes during a flight. Using calibrated secondary standards from the Carbon Cycle Division of CMDL in ground based checks [*Dlugokencky et al.*, 1994], showed that the calibration curve was linear for CH_4 but had a large positive intercept of ~400 ppb as a result of interference from the oxygen peak of the sample. Thus the single-point calibration standard of 600 ppb was not sufficient to establish the calibration curve for CH_4. Values of CH_4 measured by ACATS in the troposphere were calibrated by using a correlation of CH_4 versus CFC-11 measurements [*Elkins et al.*, 1993; *Dlugokencky et al.*, 1994] from the CMDL cooperative flask station at Niwot Ridge, Colorado (40.05°N, 105.59°W, altitude 3472 m). The station resides in the midtroposphere at nearly the same latitude as Moffett Field, California (37°N, altitude 30 m). The calibration scales for CFC-11 and CFC-113 were established by comparing the instrumental response to the gravimetric standards prepared by similar techniques described in *Novelli et al.*, [1991]. The stability of the CFC-11 scale is described in *Elkins et al.*, [1993].

The other measurements used here are described in the following: from the ATLAS tunable diode laser (TDL) spectrometer [*Lowenstein et al.*, 1990, 1993] from the ALIAS TDL spectrometer [*Webster et al.*, 1994]; from the Harvard Lyman α/OH fluoresence instrument [*Hinsta et al.*, 1994]; from balloonborne frost-point hygrometers [*Oltmans*, 1985]; and H_2O from the AL Lyman α/OH fluoroescene instrument [*Kelly et al.*, 1989]. The sampling of these instruments is typically 1 Hz. For use here, the data were averaged for 20 seconds before each ACATS sample, except for ATLAS N_2O that was averaged for 10 seconds. As a comparison, the AASE-II measurements CFC-11 and -113 from ACATS are included here. The AASE-II measurements and their correlation are discussed in *Woodbridge et al.*, [1995]. Measurements of CH_4 collected from flask samples using the Whole Air Sampler during AASE-II are also included [*Schauffler et al.*, 1993].

Results

During SPADE, ACATS provided measurements of CFC-11 on ten flights (November 9 and 12, 1992; April 30, May 1, 3, 6, 7, 12, 14, and 18, 1993, 1215 data points) of CFC-113 on nine flights (November 12, 1992; April 30, May 1, 3, 6, 7, 12, 14, and 18, 1993, 1117 points), and CH_4 on eight flights (April 30, May 1, 3, 6, 7, 12, 14, and 18, 1993, 970 points).

Perhaps the most interesting individual flight during the SPADE campaign was that of May 7, 1993 (see Figure 5.19). The ER-2 ascended to a cruising altitude of about 20 km (7.5 kPa) and operated in racetrack patterns such that the plane sampled the same locations several times. Three distinct levels of mixing ratios can be seen in the ACATS data. Ambient tropospheric levels of CH_4 and CFC-11 are observed during the ascent and descent. During the ascent the high CH_4 measurements (CH_4 > 1.80 ppm) were attributed to polluted air above the San Francisco Bay area. Midlatitude and polar stratospheric vortex mixing ratios were measured during the main portion of the flight. The higher mixing ratios (CH_4 ~1.40 ppm and CFC-11 ~140 ppt), immediately following the ascent and

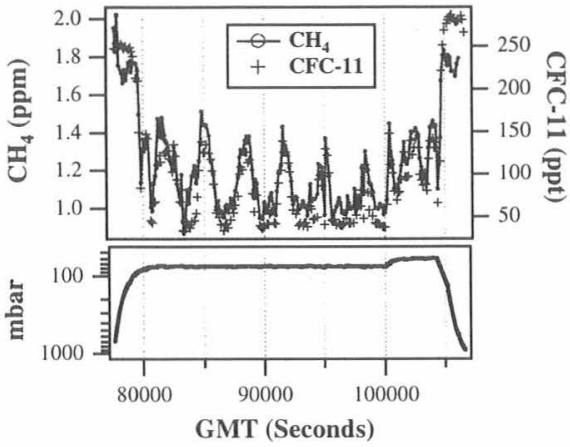

Fig. 5.19. ACATS CH_4 and CFC-11 mixing ratios measured during the flight of May 7, 1993, with accompanying pressure profile. Tropospheric measurements were observed on the ascent and descent. Two distinct air pacels with constant mixing between the air parcels were encountered in the lower stratosphere (20 km, about 7.5 kPa) as the plane repeatedly circled through the same location.

throughout the constant altitude portion of the flight, are typical of midlatitude lower stratospheric air. Similar mixing ratios were measured throughout the SPADE campaign (see Figure 5.20 for complete ACATS SPADE data) and AASE-II. The low mixing ratios (CH_4 < 1.00 ppm and CFC-11 < 50 ppt) are levels consistent with polar vortex air measurements made during AASE-II. The polar air parcel was located near the Pacific coast (north of 37°N and west of 123.75°W) and was encountered eight separate times.

Comparison of the ACATS tracers measured during AASE-II and SPADE shows that the May 7 flight does not obey the same correlations as the remaining data, especially the CFC-11 data (Figure 5.20). This flight exhibits a breakdown in slope equilibrium where mixing between the two air parcels has not had enough time to mix along global mixing ratio isopleths. Since there is mixing between two distinctly different air parcels, a linear fit intersects the original correlation at two points, namely the initial midlatitude and polar air mixing ratios.

Figure 5.20 shows the various SPADE correlations between the long-lived tracers and the May 7 flight displayed with a plus (+) symbol. The thick, solid lines are least-square fits to the combined data sets from AASE II and SPADE: the fit spans only the range of measured mixing ratios. The two missions can be usefully combined since there was only a short time span between the missions, growth rates of the species in the stratosphere have not changed significantly, and the missions were conducted at comparable latitudes. Drawing a linear fit through this flight (excluding the tropospheric values), the initial polar vortex CFC-11 mixing ratio can be inferred as 11 ± 5 ppt, CFC-113 as 8 ± 8 ppt, CH_4 as 870 ± 50 ppb, and N_2O as 90 ± 10 ppb. These mixing ratios are indicative of higher stratospheric air that has gone through vertical descent over the polar region, typical of values seen during AASE-II.

The correlations of CFC-11 versus N_2O and CH_4 are the most affected and may be related to the relative lifetimes of the tracers. The linear portion of the correlation plots in Figure 5.20, excluding data from May 7, can be used to calculate the stratospheric lifetime of the species, if slope equilibrium is obeyed and the ratio of the gradients of the species are nearly constant (a necessary condition for linearity) [*Plumb and Ko*, 1992]. Potential temperature (θ) values below 430 K were excluded to filter tropospheric values from the data. Using the arguments of *Plumb and Ko* [1992] for calculating steady-state lifetimes the linear relationship between two tracers can be expressed as:

$$\tau_1/\tau_2 = (\sigma_1/\sigma_2)(d\sigma_2/d\sigma_1) \qquad (1)$$

where τ_1 and τ_2 are the stratospheric lifetimes as defined as the mass of the compound in the total atmosphere divided by the stratospheric loss, σ_1 and σ_2 are mixing ratios of specie 1 and 2, and $d\sigma_2/d\sigma_1$ is the the slope of the linear correlation between the species. Since the growth rates of CFC-11 [*Elkins et al.*, 1993] and CH_4 [*Dlugokencky et al.*, 1994] have decreased to near zero, and the growth rate of N_2O is small (0.2-0.3% yr^{-1}), steady state can be assumed.

The fit through the CH_4 and CFC-11 correlation (containing 1013 points) is σ_{CH_4} (ppm) =(0.0029 ± 0.0001)*$\sigma_{CFC\text{-}11}$(ppt) + (1.02 ± 0.01), where σ_{CH_4} and $\sigma_{CFC\text{-}11}$ are the mixing ratios of each tracer. CFC-11 has no significant tropospheric sink. The stratospheric lifetime is equivalent to the atmospheric lifetime estimated to be 55 ± 8 years [*Elkins et. al.*, 1993]. The CFC-11 lifetime is the best known of all tracers measured during SPADE, because the industrial emissions are known to better than ±5% and because an extensive set of worldwide measurements exists for CFC-11. The calculated stratospheric CH_4 lifetime is then 129 ± 20 years and compares well with the lifetime of 147 years estimated by *WMO* [1991]. The large uncertainty in the calculations is proportionally divided between the uncertainty in the CFC-11 lifetime, mass of the atmosphere, the uncertainty in the mixing ratios, and a small contribution from the error in the slope.

Nitrous oxide was used as a stratospheric tracer because of its long lifetime and relatively small growth rate. The most reliable and consistent N_2O data from the AASE-II and SPADE campaigns was provided by the ATLAS instrument [*Loewenstein et al.*, 1993]. Using CFC-11 as a lifetime standard in eq. 1 and the asymptotic linear slope near the tropopause, [σ_{N_2O} (ppb) = 0.662 ± 0.006) $\sigma_{CFC\text{-}11}$ + (143.7 ± 0.7) 2100 points] a stratospheric lifetime of 106 ± 16 years was calculated.

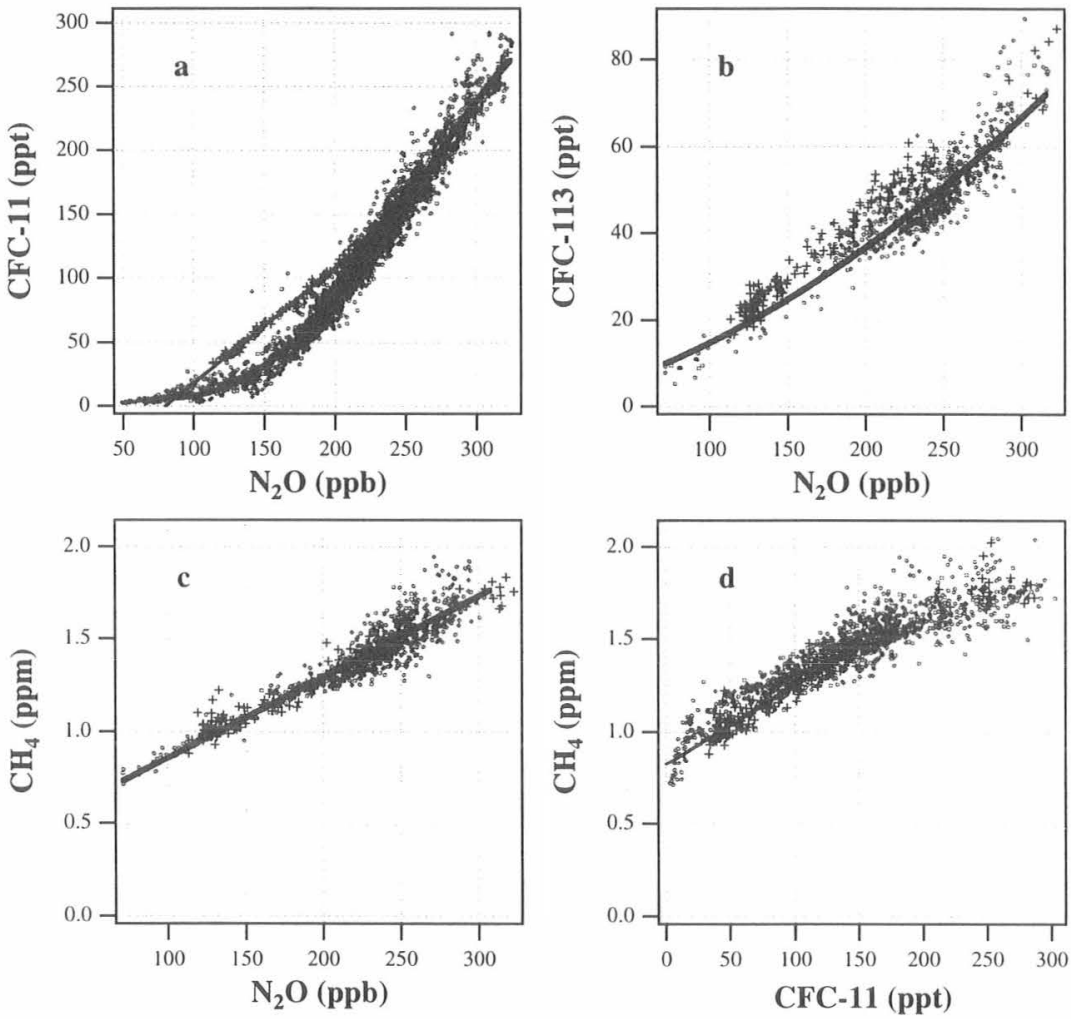

Fig. 5.20. Correlations between ACATS species for (*a*) CFC-11, (*b*) CFC-113, (*c*) CH_4 versus ATLAS N_2O, and (*d*) ACATS CH_4 versus ACATS CFC-11. The squares (□) are data for all of the ACATS SPADE flights excluding May 7, 1993, which are shown as the pluses (+). The solid lines are least squares fits through the same species by combining data from the AASE-II and SPADE missions. Both Figures 5.20*a* and *d* show considerable deviation, with respect to the flight on May 7, from the combined mission fit. This is probably the result of rapid mixing between two distinct air parcels originating from the midlatitudes and the polar regions.

Since there are no significant tropospheric sinks for N_2O, this value is also equal to the atmospheric lifetime. In contrast, higher estimates are reported yielding 132 years and 170 years by *WMO* [1991] and by *Prinn et al.*, [1990] respectively, where the latter use inverse method calculations and global tropospheric data from N_2O. Based on new absorption cross sections for O_2 in the Schumann-Runge band, *Ko et al.*, [1991] calculate an atmospheric lifetime of 110 years using vertical profiles of N_2O from satellites and *Minschwaner et al.*, [1993] calculate a lifetime of 123 ± 20 years from balloon measure-ments. These results are in support of the more recent, shorter lifetime estimates.

During the SPADE campaign, both ACATS and the TDL spectrometer, ALIAS [*Webster et al.*, 1994], were measuring CH_4. A comparison between the two measurements for θ>430 K, gives a fit ALIAS σ_{CH_4} (ppm) = (0.86 ± 0.04) * ACATS σ_{CH_4} + (0.03 ± 0.03)(ppm) (r^2 = 0.8516), where the average residual standard deviation of the fit is 0.1 ppm. This discrepancy is not within the stated experimental error limits of the ALIAS (5-10%) and ACATS (7%)

instruments, and is surprising since a comparison of laboratory standards is within the errors [*Webster et al.*, 1994]. The comparison between ACATS CH_4 and CFC-11 shows tropospheric mixing ratios of the two species agree with those from the CMDL network (σ_{CH_4} = 1.75 ppm and $\sigma_{CFC\text{-}11}$ = 270 ppt). The ALIAS data would give a considerably lower value of 1.52 ppm for tropospheric CH_4. Since ALIAS relies on spectroscopic parameters for calibration and not in-flight calibration, an error in either the line strength or air-broadening coefficients could be responsible for this difference. Therefore, the ACATS values were used for CH_4 for this work.

The dominant sink for stratospheric CH_4 is from oxidation by the hydroxyl radical (OH) [see *Le Texier et al.*, [1988]). As CH_4 is oxidized, both H_2O and H_2 are produced. Molecular hydrogen is subsequently oxidized to H_2O. The rate and efficiency at which CH_4 oxidizes and the rate the remaining H_2 is oxidized lends to the production efficiency of H_2O from CH_4. In the midlatitude lower stratosphere, H_2 is produced more rapidly than H_2O and the rate at which H_2 oxidizes is slower than the CH_4 rate. Thus, the H_2 oxidation is not concurrent with CH_4 oxidation, leading to a local H_2O production expressed as dH_2O/dCH_4 of less than 2.0. Mixing with dehydrated air (occurs more often in the southern hemisphere) and mixing with low water vapor air parcels can also yield a lower production. Figure 5.21 shows three different H_2O measurements: Harvard H_2O measurements on the ER-2 aircraft, AL measurements on the ER-2 aircraft, and CMDL measurements on balloons at a nearby location, Crow's Landing, California, plotted against ACATS CH_4 conducted during SPADE. The slope of each line gives the production that ranges from -0.8 ± 0.4 for the CMDL H_2O measurements, -1.34 ± 0.04 for AL H_2O measurements, and -1.77 ± 0.04 for the Harvard H_2O measurements. The difference between the production of H_2O cannot be the result of the CH_4 measurements since ACATS agrees well with previous CH_4 measurements of Whole Air Sampler [*Schauffler et al.*, 1993] versus AL H_2O during AASE-II (Figure 5.21). Correlation of ALIAS CH_4 with Harvard H_2O yields a slight increase in the production of H_2O (-2.28 ± 0.04) that is higher than the theoretical value at this altitude [*Le Texier et al.*, 1988]. While arguments were made by *Dessler et al.* [1994] that the production should be near 2, the absolute value of Harvard H_2O is also higher than the two other H_2O measurements.

Conclusions

Slope equilibrium is generally obeyed in the polar regions and midlatitudes at the altitudes (0-21 km) covered by the ER-2 aircraft. An exception occurs after the breakup of the polar vortex and its subsequent mixing with the midlatitudes when quasi-horizontal mixing is not fast enough to establish the original slope equilibrium. If the lifetime of one tracer is much less than the lifetime of the second tracer, a new slope on the cross-plot is established that is maintained by conservative mixing between the two air parcels. If the application of CFC-11 as a stratospheric lifetime standard is valid and slope equilibrium is obeyed, then based on the measurements presented here, the calculated lifetime of N_2O is shorter (106 ± 16 years) than previously estimated (150-170 years) by examining tropospheric N_2O budgets. Unless an unknown tropospheric sink exists, there could be large missing sources as high as 50% of the total N_2O source that remain unaccounted for in the inventory of sources.

5.2.2. Automated Four-Channel Field Gas Chromatographs

The NOAH Division continued to build and test the newest generation of four-channel GCs. These instruments are designed to make frequent, automated measurements of radiatively important and halogenated trace gases. The deployment of four-channel GCs at existing CMDL observatories (BRW, MLO, SMO, and SPO), the NWR cooperative site, and new field sites at WITN tower (North Carolina), Harvard Forest (Massachusetts), and Alert, Canada, will expand both the geographical coverage of trace gas monitoring and the number of species measured.

Features

Much of the technology found in the new generation of field GCs has evolved through the development of compact, lightweight, automated GCs for in situ trace gas analysis aboard the ER-2 aircraft. Thus, the field GCs are very compact and modular with each channel having its own 12-port gas sampling valve, chromatographic column pair, ECD, and electrometer. If a component requires maintenance or repair, it can effectively be removed and replaced without disrupting measurements on the other channels.

The control and acquisition software for the instrument runs on a conventional IBM-compatible personal computer with a 80486 CPU. The control and data acquisition hardware within the GC consists of a 96-channel analog-to-digital (A/D) board, a digital I/O board, and a dedicated four-channel A/D board for logging ECD signal data. The run program includes on-screen display of chromatograms and pertinent engineering data such as component and zone temperatures, sample loop flow rate and pressure, carrier gas flow rates, carrier gas and calibration gas tank pressures, and the relative humidity of the sample stream. A new and extremely useful feature of the run program is the real-time integration of peaks, which permits a "quick look" at data and aids in troubleshooting.

Using an eight-port stream selection valve, several ambient air streams and calibration gas flows can be sampled and analyzed in a user-defined sequence. Ambient air streams are dried through Nafion tubing to

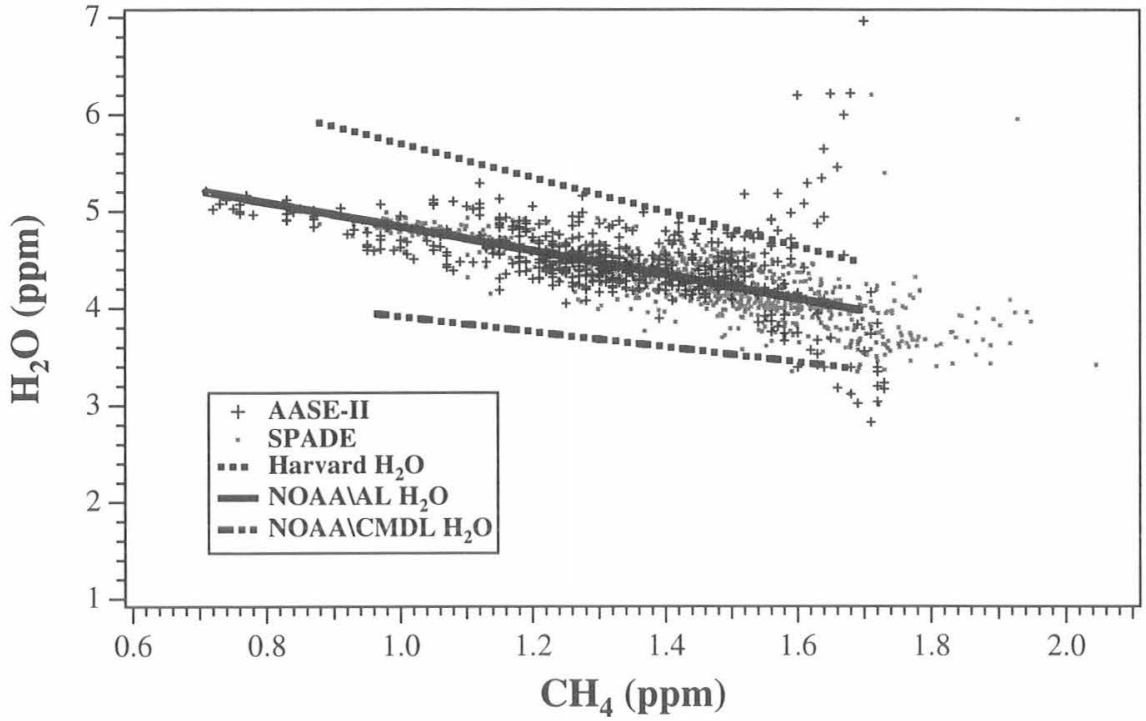

Fig. 5.21. Methane and water vapor correlations can be used to estimate the production efficiency at which CH_4 is oxidized to H_2O. The solid line is a linear fit (y = -1.24*x + 6.08) through the combined AASE-II (+) and the SPADE (•) missions over the range CH_4 <1.7 ppm. The absolute value of the slope is the production efficiency. The top dashed line is a similar fit (y = -1.77*x + 7.45) using the SPADE Harvard H_2O. The bottom dashed line is y = -0.8x + 4.7 for ACATS CH_4 versus CMDL H_2O.

a dewpoint of -25°C before analysis. The four sample loops are pressure-controlled using a pressure sensor and valve feedback system.

Each column pair, ECD, mass flow controller and sample loop is isothermally maintained by proportional, integral, derivative algorithm temperature controllers. Temperature data are logged to disk by an RS-485 loop between the temperature controllers and the computer, and controller setpoints can be changed from the keyboard. Column pairs and ECDs are encapsulated in well-insulated, cylindrical ovens 13 cm in diameter and 18 cm high that provide excellent temperature stability (1 s.d., ± 0.1°C).

There are currently five possible channels for implementation in these four-channel automated gas chromatographs. The more pertinent chromatography parameters for each channel are listed in Table 5.3. These include column dimensions (o.d. × length) and packing materials, sample loop sizes, special detection methods employed (if any), species measured, and the precision of measurement of each specie at its mixing ratio in high-pressure tanks of Niwot Ridge air.

Work will begin in 1994 to utilize the sample loop pressure control for "pressure-calibrations," the injection of different pressures of a calibration gas to generate calibration curves. Pressure-calibration curves show little nonlinearity over a pressure range of 15% (90% to 105% of a given setpoint). If satisfactory results can be obtained through this method, the need for having several calibration tanks at a given site will be eliminated.

TABLE 5.3. Pertinent Chromatography Parameters for Each Channel of New Automated Field GC, Species Measured, and Precision of Measurements

Parameter	Description
	Channel 1
Precolumn	3.175 mm × 2.0 m unibeads 1S
Main column	3.175 mm × 4.0 m molecular sieve 5A
Sample size	5 cm^3
Detector	N_2O-doped ECD
Species measured:	*Precision:*
H_2	0.6%
CH_4	0.4%
CO	1.0%
	Channel 2
Precolumn	3.175 mm × 1.5 m unibeads 2S
Main column	3.175 mm × 2.5 m unibeads 2S
Sample size	2.5 cm^3
Detector	ECD
Species measured:	*Precision:*
CFC-12	0.2%
CFC-11	0.2%
CFC-113	2.8%
	Channel 3
Precolumn	3.175 mm × 2.0 m OV-101 (20%)
Main Column	3.175 mm × 5.0 m OV-101 (20%)
Sample size	5.0 cm^3
Detector	ECD
Species measured:	*Precision:*
CFC-11	0.2%
CFC-113	0.5%
Chloroform	5%
Methyl chloroform	0.5%
Carbon tetrachloride	0.5%
Trichloroethylene	Unknown
Perchloroethylene	1.5%
	Channel 4
Precolumn	4.7625 mm × 2.0 m Porapak Q
Main Column	4.7625 mm × 3.0 m Porapak Q
Sample size	15.0 cm^3
Detector	ECD
Species measured:	*Precision:*
N_2O	0.2%
SF_6	1.2%
	*Channel 5**
Trap no. 1	3.175 mm × 0.040 m unibeads 1S
Trap no. 2	3.175 mm × 0.024 m Porapak Q
Precolumn	3.175 mm × 0.5 m unibeads 2S
Main column	3.175 mm × 1.0 m unibeads 2S
Sample size	40.0 cm^3
Detector	O_2-doped ECD
Species measured:	*Precision:*
HCFC-22	2.8%

*Samples are first pre-concentrated on trap no. 1 cooled to -50°C. Species of interest are desorbed from this trap by heating to 110°C, then are focused on trap no. 2 cooled to -50°C. Trap no. 2 is rapidly heated to 110°C just prior to injection.

5.3. REFERENCES

AFEAS (Alternative Fluorocarbons Environmental Acceptability Study), *Historic production, sales and atmospheric release of HCFC-142b*, Washington, D.C., USA, 1994.

Braker, W., and A.L. Mossman, *Matheson Gas Data Book*, Sixth Edition, 711 pp., Matheson Gas Products, Secaucus, NJ, 1980.

Butler, J.H., J.W. Elkins, B.D. Hall, S.O. Cummings, and S.A. Montzka, A decrease in the growth rates of atmospheric halon concentrations, *Nature, 359*,403-405,1992.

Collins, J.E., Jr., G.W. Sachse, B.E. Anderson, A.J. Weinheimer, J.G. Walega, and B.A. Ridley, AASE-II in situ tracer correlations of methane, nitrous oxide, and ozone as observed aboard the DC-8, *Geophys. Res. Lett., 20(22)*, 2543-2546, 1993.

Dessler, A.E., E.M. Weinstock, E.J. Hintsa, J.G. Anderson, C.R. Webster, R.D. May, J.W. Elkins, and G.S. Dutton, An examination of the total hydrogen budget of the lower stratosphere, *Geophys. Res. Lett., 21(23)* 2563-2566, 1994.

Dlugokencky, E.J., K.A. Masarie, P.M. Lang, P.P. Tans, L.P. Steele, and E.G. Nisbet, A dramatic decrease in the growth rate of atmospheric methane in the northern hemisphere during 1992, *Geophys. Res. Lett., 21(1)*, 45-48, 1994.

Elkins, J.W., T.M. Thompson, T.H. Swanson, J.H. Butler, B.D. Hall, S.O. Cummings, D.A. Fisher, and A.G. Raffo, Decrease in the growth rates of atmospheric chlorofluorocarbons 11 and 12, *Nature, 364*, 780-783, 1993.

EPA (Environmental Protection Agency), Protection of stratospheric ozone, *Federal Register, 58*, 15,014-15,048, 1993.

Goldan, P.D., F.C. Fehsenfeld, and J.P. Phillips, Detection of carbon monoxide at ambient levels with an N_2O-sensitized electron-capture detector, *J. Chromatogr., 239*, 115-126, 1982.

Hintsa, E. J., E.M. Weinstock, A.E. Dessler, and J.G. Anderson, SPADE H_2O measurements and the seasonal cycle of stratospheric water vapor, *Geophys. Res. Lett., 21(23)*, 2559-2562, 1994.

Kawa, S.R., D.W. Fahey, L.E. Heidt, W.H. Pollock, S. Solomon, D.E. Anderson, M. Loewenstein, M.H. Proffitt, J.J. Margitan, and K.R. Chan, Photochemical partitioning of the reactive nitrogen and chlorine reservoirs in the high-latitude stratosphere, *J. Geophys. Res., 97(D8)*, 7905-7923, 1992.

Kelly, K.K., A.F. Tuck, D.M. Murphy, M.H. Proffitt, D.W. Fahey, R.L. Jones, D.S. McKenna, M. Loewenstein, J.R. Podolske, S.E. Strahan, G.V. Ferry, K.R. Chan, J.F. Vedder, G.L. Gregory, W.D. Hypes, M.P. McCormick, E.V. Browell, and L.E. Heidt, Dehydration in the lower Antarctic stratosphere during late winter and early spring, 1987, *J. Geophys. Res., 94*, 11,317-11,357, 1989.

Ko, M.K.W., N.D. Sze, and D.K. Weisenstein, Use of satellite data to constrain the model-calculated atmospheric lifetime for N_2O: Implications for other trace gases, *J. Geophys. Res., 96(D4)*, 7547-7552, 1991.

Le Texier, H., S. Solomon, and R.R. Garcia, The role of molecular hydrogen and methane oxidation in the water vapor budget of the stratosphere, *Q.J.R. Meteorol. Soc., 114*, 281-295, 1988.

Loewenstein, M., J.R. Podolske, and S.E. Strahan, ATLAS instrument characterization: Accuracy of the AASE and AAOE nitrous oxide data sets, *Geophys. Res. Lett., 17*, 481-484, 1990.

Loewenstein, M., J.R. Podolske, D.W. Fahey, E.L. Woodbridge, P. Tin, A. Weaver, P.A. Newman, S.E. Strahan, S.R. Kawa, M.R. Schoeberl, and L.R. Lait, New observations of the NO_y/N_2O correlation in the lower stratosphere, *Geophys. Res. Lett., 20(22)*, 2531-2534, 1993.

Minschwaner, K., R.J. Salawitch, and M.B. McElroy, Absorption of solar radiation by O_2: Implications for O_3 and lifetimes of N_2O, $CFCl_3$, and CF_2Cl_2, *J. Geophys. Res.*, *98(D6)*, 10,543-10,561, 1993.

Montzka, S.A., J.W. Elkins, J.H. Butler, T.M. Thompson, W.T. Sturges, T.H. Swanson, R.C. Myers, T.M. Gilpin, T.J. Baring, S.O. Cummings, G.A. Holcomb, J.M. Lobert, and B.D. Hall, in *Climate Monitoring and Diagnostics Laboratory No. 20: Summary report 1991*, pp. 60-81, edited by E.E. Ferguson and R.M. Rosson, NOAA Environmental Research Laboratories, Boulder, CO, 1992.

Montzka, S.A., R.C. Myers, J.H. Butler, J.W. Elkins, and S.O. Cummings, Global tropospheric distribution and calibration scale of HCFC-22, *Geophys. Res. Lett., 20*, 703-706, 1993.

Montzka, S.A., R.C. Myers, J.H. Butler, and J.W. Elkins, Early trends in the global tropospheric abundance of hydrochlorofluorocarbon-141b and -142b, *Geophy. Res. Lett., 21(23)*, 2483-2486, 1994*a*.

Montzka, S.A., R.C. Myers, J.H. Butler, J.W. Elkins, and S.O. Cummings, Atmospheric measurements of HCFC-22 at the South Pole, *Ant. J. U. S., 28(5)*, 267-269, 1994*b*.

Novelli, P.C., J.W. Elkins, and L.P. Steele, The development and evaluation of a gravimetric reference scale for measurements of atmospheric carbon monoxide, *J. Geophys. Res., 96(D7)*, 13,109-13,121, 1991.

Oltmans, S.J., Measurements of water vapor in the stratosphere with a frostpoint hygrometer, *Proceedings of 1985 International Symposium on Moisture and Humidity*, pp. 251-258, Instrument Society of America, Washington, DC, 1985.

Plumb, R.A., and M.K.W. Ko, Interrelationships between mixing ratios of long-lived stratospheric constituents, *J. Geophys. Res., 97*, 10,145-10,156, 1992.

Pollock, W.H., L.E. Heidt, R.A. Lueb, J.F. Vedder, M.J. Mills, and S. Solomon, On the age of stratospheric air and ozone depletion potentials in polar regions, *J. Geophys. Res., 97(D12)*, 12,993-12,999, 1992.

Prather M., and C.M. Spivakovsky, Tropospheric OH and the lifetimes of hydrochlorofluorocarbons, *J. Geophys. Res., 95(D11)*, 18,723-18,729, 1990.

Prinn, R., D. Cunnold, R. Rasmussen, P. Simmonds, F. Alyea, A. Crawford, P. Fraser, and R. Rosen, Atmospheric emissions and trends of nitrous oxide deduced from 10 years of ALE-GAGE data, *J. Geophys. Res., 95(D11)*, 18,369-18,385, 1990.

Schauffler, S.M., L.E. Heidt, W.H. Pollock, T.M. Gilpin, J.F. Vedder, S. Solomon, R.A. Lueb, and E.L. Atlas, Measurements of halogenated organic compounds near the tropical tropopause, *Geophys. Res. Lett., 20(22)*, 2567-2570, 1993.

Schauffler, S.M., W.H. Pollock, E. L. Atlas, L.E. Heidt, and J.S. Daniel, Atmospheric distributions of HCFC-141b, *Geophys. Res. Lett.*, in press, 1995.

Solomon, S., and D. Albritton, Time-dependent ozone depletion potentials for short- and long-term forecasts, *Nature, 357*, 33-37, 1992.

Solomon, S., M. Mills, L.E. Heidt, W.H. Pollock, and A.F. Tuck, On the evaluation of ozone depletion potentials, *J. Geophys. Res. 97(D1)*, 825-842, 1992.

Steele, L.P., P.J. Fraser, R.A. Rasmussen, M.A.K. Khalil, T.J. Conway, A.J. Crawford, R.H. Gammon, K.A. Masarie, and K.W. Thoning, The global distribution of methane in the troposphere, *J. Atmos. Chem., 5*, 125-171, 1987.

Swanson, T.H., J.W. Elkins, J.H. Butler, S.A. Montzka, R.C. Myers, T.M. Thompson, T.J. Baring, S.O. Cummings, G.S. Dutton, A.H. Hayden, J.M. Lobert, G.A. Holcomb, W.T. Sturges, and T.M. Gilpin, in *Climate Monitoring and Diagnostics Laboratory No. 21: Summary report 1992*, 59-75, edited by J.T. Peterson and R.M. Rosson, NOAA Environmental Research Laboratories, Boulder, CO, 1993.

UNEP (United Nations Environment Programme), *Montreal Protocol 1991 Assessment: Report of the Technology and Economic Assessment Panel*, December, 1991.

UNEP (United Nations Environment Programme), *Montreal Protocol 1993 Report of the Technology and Economic Assessment Panel,* July 1993.

Webster, C.R., R.D. May, C.A. Trimble, R.G. Chave, and J. Kendall, Aircraft laser infrared absorption spectrometer (ALIAS) for in situ stratospheric measurements of HCl, N_2O, CH_4, NO_2, and HNO_3, *Appl. Opt., 33(3)*, 454-472, 1994.

Woodbridge, E.L., J.W. Elkins, D.W. Fahey, L.E. Heidt, S. Solomon, T.J. Baring, T.M. Gilpin, W.H. Pollock, S.M. Schauffler, E.L. Atlas, M. Loewenstein, J.R. Podolske, C.R. Webster, R.D. May, J.M. Gilligan, S.A. Montzka, K.A. Boering, and R.J. Salawitch, Estimates of total organic and inorganic chlorine in the lower stratosphere from in situ and flask measurements during AASE II, *J. Geophys. Res.*, in press, 1995.

WMO (World Meteorological Organization), Scientific assessment of ozone depletion: 1991, *WMO Global Ozone Res. and Monitoring Proj. Rep. 25*, WMO Global Ozone Research and Monitoring Project, Geneva, Switzerland, 1991.